Preprints of the 21st IFAC World Congress (Virtual)
Berlin, Germany, July 12-17, 2020

Sensor Bias Fault Diagnosis for a Class of Nonlinear Uncertain Hybrid Systems

Constantinos Heracleous, Christodoulos Keliris, Christos G. Panayiotou, Marios M. Polycarpou

KIOS Research and Innovation Center of Excellence (CoE), and Department of Electrical and Computer Engineering, University of Cyprus, Nicosia, Cyprus (e-mail: con.heracleous@gmail.com; keliris.chris@gmail.com; christosp@ucy.ac.cy; mpolycar@ucy.ac.cy).

Abstract: This paper presents a sensor bias fault diagnosis approach for a class of hybrid systems with nonlinear uncertain discrete-time dynamics, measurement noise, and autonomous and controlled mode transitions. The proposed approach uses an observer based on a modified hybrid automaton framework and a fault detection scheme that employs a filtering method tighter mode-dependent thresholds for the detection of sensor faults (even with small magnitude). An autonomous guard events identification (AGEI) module is also developed and linked with both the fault detection scheme and the hybrid observer to eliminate any false alarms due to autonomous mode transitions and allow effective mode estimation. Finally, an adaptive sensor fault estimation scheme is included, which is activated once a fault is detected to isolate and estimate the sensor bias fault magnitude.

Keywords: Hybrid systems, fault diagnosis, bias sensor faults, filtering, adaptive estimation.

1. INTRODUCTION

Modern complex engineering systems consist of discrete operating modes, with each having its time-driven dynamics, thus are best represented as hybrid systems (see Daigle et al. (2016); Heracleous et al. (2017)). As a result, fault diagnosis methods, that help keep these systems running smoothly, must take into account the combined discrete-event and time-driven dynamics to be effective. This poses a significant challenge since it requires the estimation of the hybrid state that consists of continuous and discrete states, and the diagnosis of faults in both dynamics parts (i.e., discrete-event and time-driven).

Various approaches have been proposed in the literature that addresses the problem of fault diagnosis in hybrid systems. Some of these approaches, such as Narasimhan and Biswas (2007); Zhao et al. (2005) are focused on diagnosing faults only in the time-driven dynamic part, while approaches such as Hofbaur and Williams (2004); Bayoudh et al. (2008) are focused on diagnosing faults only the discrete-event dynamic part. Some other approaches, such as Cocquempot et al. (2004); Wang et al. (2007); Heracleous et al. (2018b), can diagnose faults in both dynamics parts. However, apart from faults in the time-driven or discrete-event dynamic parts, a significant issue is the occurrence of sensor faults, since they may affect the functionality of automation and supervision schemes and cause wrong decisions and disorientation of corrective actions (see Reppa et al. (2014)). Although various methodologies have been developed that deal with the sensor fault diagnosis problem in time-driven dynamical systems, such as Vemuri (2001); Zhang et al. (2005); Reppa et al. (2014); Keliris et al. (2018), the research conducted for sensor fault diagnosis in hybrid systems is still minimal according to the authors' knowledge. Specifically, the problem of sensor bias fault diagnosis in hybrid systems with autonomous mode transitions is challenging since the sensor bias fault can cause the wrong estimation of the system mode and subsequently, the triggering of false alarms and also the failure to isolate the fault successfully.

Thus, the primary objective and main contribution of this paper is the design of a sensor bias fault diagnosis approach for a class of hybrid systems with nonlinear uncertain discrete-time dynamics, measurement noise, and autonomous and controlled mode transitions. The proposed approach uses a hybrid automaton observer that prevents the need for pre-enumeration of all modes in a system level, while the fault detection scheme employs a filtering approach to attenuate the effect of measurement noise and allow tighter detection thresholds. An important part of the fault diagnosis approach is the development of a more improved version of the autonomous guard events identification (AGEI) module that introduced in our previous work in Heracleous et al. (2018a). The AGEI module eliminates any false alarms due to autonomous mode transitions by calculating and setting a new detection threshold promptly in the fault detection scheme. Moreover, it can identify when an autonomous mode transition occurred in the system and trigger it in the observer allowing effective mode estimation. Finally, an adaptive sensor fault estimation scheme is implemented and activated once a fault is detected. The scheme can estimate the sensor bias fault magnitudes that are used for fault isolation purposes and also by the observer through a simple accommodation strategy to compensate the measurements so that both the observer and AGEI module continue their correct operation.

2. PROBLEM FORMULATION

We consider a hybrid system $\mathcal{S}$ that consists of N subsystems $\mathcal{A}_I$, $I \in \{1, \ldots, N\}$, with each having several modes of operation. The individual subsystems are modeled as *open hybrid automata (OHA)*, while the overall system is the composition of those automata that operate in parallel and interact via shared variables. We refer to the model for the overall system as *composition Open Hybrid Automaton (cOHA)*. Fig. 1 illustrates an example of a *cOHA* composed of two *OHAs* that interact via shared variables.

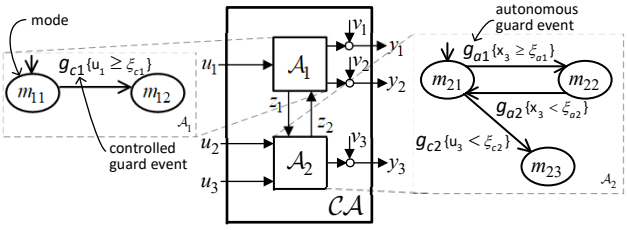

Fig. 1. Example of a *cOHA* composed of two *OHAs*.

Each subsystem *OHA* can be seen as an extension of a finite-state machine (FSM) that incorporates nonlinear uncertain discrete-time difference and algebraic equations for each mode to capture the time-driven dynamic evolution of a subsystem. More specifically, based on Hofbaur and Williams (2004); Heracleous et al. (2018b), we describe the *OHA* for the subsystem A_I, $I \in \{1, \ldots, N\}$ as a tuple

$$\mathcal{A}_I := \langle \mathbf{s}_I, Q_I, \mathbf{w}_I, F_I, \eta_I, \Sigma_I, \gamma_I, S_{I,0} \rangle \tag{1}$$

where [1] :

- $\mathbf{s} = \{q\} \cup \mathbf{x}$ is the hybrid state, composed of the operation mode (discrete state) $q \in Q$ and the continuous state variables $\mathbf{x} \in \mathbb{R}^{n^x}$,
- $Q = \{m_1, \ldots, m_{N_q}\}$ specifies a finite set of N_q operation modes,
- $\mathbf{w} = \mathbf{u} \cup \mathbf{z} \cup \mathbf{y}$ is the set of I/O variables, that aggregates the inputs $\mathbf{u} \in \mathbb{R}^{n^u}$, the shared variables $\mathbf{z} \in \mathbb{R}^{n^z}$ that models the interconnections with other subsystems, and the outputs $\mathbf{y} \in \mathbb{R}^{n^y}$,
- $F : Q \mapsto F_{DE} \cup F_{AE}$ specifies the time-driven dynamics evolution in terms of nonlinear discrete-time difference equations F_{DE} (with sampling-period T_s) and algebraic equations F_{AE}, where both incorporate the effects of *local uncertainty* η_I,
- $\Sigma = G_a \cup G_c$ is a set of events that consists of: (a) *autonomous* guard events $g_a \in G_a \subset \Sigma$ where each is triggered by a continuous state value x based on an enabling condition of the form $x \ \triangle \ \xi_a$, with $\xi_a \in \mathbb{R}$ and $\triangle \in \{\leq, \geq, =, <, >\}$, (b) *control* guard events $g_c \in G_c \subset \Sigma$ where each is triggered by an input variable u value, based on an enabling condition of the form $u \ \triangledown \ \xi_c$, with $\xi_c \in \mathbb{R}$ and $\triangledown \in \{\leq, \geq, =, <, >\}$,
- $\gamma : Q \times \Sigma \to Q$ are the transition functions labeled by autonomous g_a or control g_c events,
- S_0 denotes the initial hybrid state $\mathbf{s}_0 = \{q_0\} \cup \mathbf{x}_0$.

[1] The components of an *OHA* $\mathcal{A}_I$ are denoted by $\mathbf{s}_I, Q_I, \mathbf{w}_I, F_I$ etc., but when there is no risk of ambiguity and for the sake of simplicity the subscripts will be omitted.

The overall system $\mathcal{S}$ is modeled by the *cOHA* $\mathcal{CA}$ that specifies the parallel composition of the set of subsystems automata $A := \{\mathcal{A}_1, \ldots, \mathcal{A}_N\}$ as a tuple

$$\mathcal{CA} := \langle A, \mathbf{u}, \mathbf{y}, \eta, \mathbf{v}, \boldsymbol{\sigma} \rangle \tag{2}$$

where $\mathbf{u} = [u_1, \ldots, u_{n^u}]^T$ are the input variables and $\mathbf{y} = [y_1, \ldots, y_n]^T$ are the output variables of *cOHA*, aggregated from each subsystem A_I to single vectors and re-indexed by the mapping functions [2] $M_u : \{1, \ldots, n_I^u\} \mapsto \{1, \ldots, n^u\}$ and $M_y : \{1, \ldots, n_I^y\} \mapsto \{1, \ldots, n\}$, respectively. η is the mode dependent nonlinear function that denotes the overall *uncertainty* of the system, which acts on the continuous states $\mathbf{x} = \mathbf{x}_1 \cup \ldots \cup \mathbf{x}_N$. The vector $\mathbf{v} \in \mathbb{R}^n$ represents the measurement noise, whilst the vector $\boldsymbol{\sigma} : \mathbb{R} \mapsto \mathbb{R}^n$ represents the sensor bias caused due to a sensor fault. The *cOHA* describes the continuous evolution of the overall system using the following set of mode-dependent difference equations with time step k ($t = T_s k$):

$$\begin{aligned} \mathbf{x}_{k+1} &= f(\mathbf{q}_k, \mathbf{x}_k, \mathbf{u}_k) + \eta(\mathbf{q}_k, \mathbf{x}_k, \mathbf{u}_k, k), \quad k = 0, 1, \ldots \\ \mathbf{y}_k &= \mathbf{x}_k + \mathbf{v}_k + \beta(k - K_0)\boldsymbol{\sigma}_k \end{aligned} \tag{3}$$

where $\mathbf{q} = \{q_1, \ldots, q_N\}$ is the system mode (as a collection of the subsystems modes $q_I \in Q_I$), and $\mathbf{x} = [x_1, \ldots, x_n]^T$ are the system continuous states aggregated from each subsystem $\mathcal{A}_I$ and re-indexed using the mapping function $M_x : \{1, \ldots, n_I^x\} \mapsto \{1, \ldots, n\}$. $f : Q \times \mathbb{R}^n \times \mathbb{R}^{n^u} \mapsto \mathbb{R}^n$ represents the mode-dependent *time-driven dynamics* of the system, and $\eta : Q \times \mathbb{R}^n \times \mathbb{R}^{n^u} \times \mathbb{N} \mapsto \mathbb{R}^n$ represents the overall mode-dependent *uncertainty* of the system. The term $\beta(k - K_0) : \mathbb{R} \mapsto \mathbb{R}$ models the time evolution of the sensor fault(s), where K_0 is the unknown discrete-time step at which the sensor fault occurs. Without loss of generality we consider all sensor faults to occur at the same step K_0. The time profile $\beta(k - K_0)$ can be used to model both abrupt and incipient faults, however, in this paper we only consider the case of abrupt sensor fault where

$$\beta(k - K_0) = \begin{cases} 0, & \text{if } k < K_0 \\ 1, & \text{if } k \geq K_0. \end{cases} \tag{4}$$

The objective of this work is to develop a fault diagnosis approach that will enable the detection and isolation of sensor bias fault(s) for the hybrid system $\mathcal{S}$, considering the presence of autonomous mode transitions, modeling uncertainty η and measurement noise $\mathbf{v}$.

The following assumptions are used throughout the paper:

Assumption 1. The hybrid systems' continuous state variables $\mathbf{x}$ belong to a compact and bounded set $\mathcal{X}$ before and after the occurrence of fault(s), that is $\mathbf{x}_k \in \mathcal{X} \ \forall \ k \geq 0$.

Assumption 2. All measurement noise components are bounded with known bounds $\bar{\nu}_i$, i.e.,: $|\nu_{i,k}| \leq \bar{\nu}_i$, for all $k \geq 0$ and all $i = 1, 2, \ldots, n$.

Assumption 3. Each component of the overall modeling uncertainty η in (3) is an unstructured and possibly unknown nonlinear function of $\mathbf{q}_k$, $\mathbf{x}_k$, $\mathbf{u}_k$, and k, but it is bounded by some known functional $\bar{\eta}_i$, i.e.,

$$|\eta_i(\mathbf{q}_k, \mathbf{x}_k, \mathbf{u}_k, k)| \leq \bar{\eta}_i(\mathbf{q}_k)$$

for all system modes $\mathbf{q}_k = \{q_{1,k}, \ldots, q_{N,k}\}$.

[2] For example in Fig. 1 the two subsystems *OHAs* each with inputs $\mathbf{u_1} = \{u_1\}$ and $\mathbf{u_2} = \{u_1, u_2\}$ will result a *cOHA* with aggregated and re-index inputs $\mathbf{u} = \mathbf{u}_1 \cup \mathbf{u}_2 \mapsto M_u[u_1, u_2, u_3]^T$ as shown.

3. FAULT DIAGNOSIS SCHEME

The proposed sensor bias fault diagnosis scheme for hybrid systems is depicted in Fig. 2. It consists of the hybrid automaton observer, the fault detection module, the autonomous guard event identification (AGEI) module, and the adaptive sensor fault estimation module. We describe each of these parts in the following paragraphs.

3.1 Hybrid Automaton Observer

The hybrid automaton observer has a similar structure to the *cOHA* in (2). Specifically, the hybrid automaton observer is a parallel composition of the set of subsystems OHAs $A := \{\mathcal{A}_1, \ldots, \mathcal{A}_N\}$ as in (1) [3] and is represented as a tuple

$$\mathcal{O} := \langle A, \mathbf{u}, \tilde{\mathbf{y}}, \boldsymbol{g}_a, \hat{\mathbf{q}}, \hat{\mathbf{x}} \rangle \tag{5}$$

where the observer inputs are the system's input vector $\mathbf{u}$, the output vector $\tilde{\mathbf{y}} \triangleq \mathbf{y} - \hat{\boldsymbol{\sigma}}$ (where $\hat{\boldsymbol{\sigma}}$ are the estimated values for the sensor bias from the adaptive sensor fault estimation module as shown in Fig. 2), and also the autonomous guards triggering events $\boldsymbol{g}_a$ provided by the AGEI module. The observer outputs are the estimates for the system mode $\hat{\mathbf{q}}$ and the continuous state $\hat{\mathbf{x}}$. Note that the estimated values for the sensor bias $\hat{\boldsymbol{\sigma}}$ become non-zero only after a fault is detected, and the adaptive sensor fault estimation module is activated. Thus, before the fault detection $\tilde{\mathbf{y}} = \mathbf{y}$ while after the fault detection $\tilde{\mathbf{y}} = \mathbf{y} - \hat{\boldsymbol{\sigma}}$. In this way, a simple fault accommodation strategy is performed by replacing the measurements $\mathbf{y}$ with the compensated measurements $\mathbf{y} - \hat{\boldsymbol{\sigma}}$. Thus, the hybrid state estimation is not affected by the sensor bias fault $\boldsymbol{\sigma}$ contained in $\mathbf{y}$ since it is canceled out by $\hat{\boldsymbol{\sigma}}$.

The main task of the hybrid automaton observer is to estimate the hybrid state $\hat{\mathbf{s}}_k = \hat{\mathbf{q}}_k \cup \hat{\mathbf{x}}_k$ at each time step k, given the initial hybrid state $\mathbf{s}_0 = \mathbf{q}_0 \cup \mathbf{y}_0$, the values for inputs $\mathbf{u}_k$ and outputs $\tilde{\mathbf{y}}_k$ of the system, as well as the autonomous guard triggering events $\boldsymbol{g}_a$ provided by the AGEI module. To achieve the task of hybrid state estimation, the observer carries out the following:

Mode estimation The observer estimates the system mode $\hat{\mathbf{q}}_k = \{\hat{q}_{1,k}, \ldots, \hat{q}_{N,k}\}$ at each time step k by:

(a) tracking transition functions that are labeled by control guard events, i.e., $\hat{q}_{I,k+1} = \gamma_I(g_{cI}, \hat{q}_{I,k})$, in each subsystem *OHA* of the hybrid automaton observer, and
(b) executing any transition functions labeled by autonomous guard events, i.e., $\hat{q}_{I,k+1} = \gamma_I(g_{aI}, \hat{q}_{I,k})$, that are triggered by the AGEI module in each subsystem *OHA* of the hybrid automaton observer.

Continuous State Estimation The hybrid automaton observer estimates the continuous state values using the following estimation model:

$$\hat{\mathbf{x}}_{k+1} = f(\hat{\mathbf{q}}_k, \tilde{\mathbf{y}}_k, \mathbf{u}_k) \tag{6}$$

where f is obtained based on the estimated system mode $\hat{\mathbf{q}}_k = \{\hat{q}_{1,k}, \ldots, \hat{q}_{N,k}\}$ as in Hofbaur and Williams (2004); Heracleous et al. (2018b) i.e., by solving

$$F(\hat{\mathbf{q}}_k) = F_1(\hat{q}_{1,k}) \cup \cdots \cup F_N(\hat{q}_{N,k}). \tag{7}$$

[3] The OHAs for the hybrid automaton observer don't include any modeling uncertainty η as in the OHAs for the system.

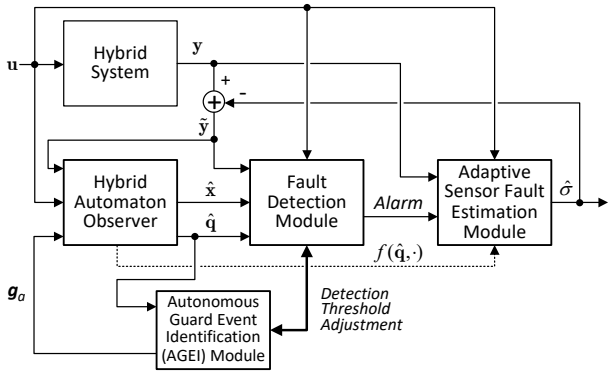

Fig. 2. Sensor bias fault diagnosis scheme for hybrid systems.

3.2 Fault Detection

The fault detection scheme utilizes the filtering approach devised in Keliris et al. (2015) for uncertain discrete-time systems and later adapted for the case of uncertain hybrid systems in Heracleous et al. (2018a). The use of filtering dampens the effect of measurement noise and allows the derivation of tighter detection thresholds, which enhances the detectability of smaller magnitude faults. We describe the fault detection scheme in the following paragraphs, and we derived analytical results regarding the detectability of sensor bias faults by the proposed scheme.

Filtering Approach To dampen the effect of measurement noise $\mathbf{v}_k$ (see (3)), each measured output variable y_i, $i = 1, \ldots, n$ is filtered by $H(z)$, where $H(z)$ is an m-th order, asymptotically stable filter (poles lie inside the open unit disc $|z| = 1$) with proper transfer function

$$H(z) = \frac{d_0 + d_1 z^{-1} + d_2 z^{-2} + \ldots + d_m z^{-m}}{1 + c_1 z^{-1} + \ldots + c_m z^{-m}}. \tag{8}$$

In general, each y_i can be filtered by a different filter, but in this paper, without loss of generality and to simplify the presentation, we consider the same $H(z)$ for all the output variables. Also, note that the form of $H(z)$ allows both IIR and FIR types of digital filters.

Based on $H(z)$, we can define the filter $H_p(z) = z^{-1}H(z)$ where $H_p(z)$ is also asymptotically stable since it comprises of the same poles as $H(z)$ with an additional pole at $z = 0$ (inside $|z| = 1$). Since the filters $H(z)$ and $H_p(z)$ (with impulse responses $h(t)$ and $h_p(t)$, respectively) are asymptotically stable, they are also BIBO stable. Thus, owing to Assumption 2, the filtered measurement noise $\mathbf{v}_{F,k} \triangleq H(z)[\mathbf{v}_k]$ is bounded as follows:

$$|v_{Fi,k}| \leq \bar{v}_{Fi,k} \quad i = 1, 2, \ldots, n, \tag{9}$$

where $\bar{v}_{Fi}$ are computable bounds. The filter $H(z)$ is selected based on the noise characteristics so that the noise is dampened.

Residual Signal Generation To generate the residual error, we first examine the results of filtering the system's output and the observer's (continuous) state estimates. Note that before a fault is detected, $\hat{\boldsymbol{\sigma}}_k = 0$ and thus $\tilde{\mathbf{y}}_k = \mathbf{y}_k$. Therefore, by filtering the output signal $\tilde{\mathbf{y}}_k$ we obtain:

$$\mathbf{w}_k \triangleq H(z)[\tilde{\mathbf{y}}_k] = H(z)[\mathbf{y}_k] = H(z)[\mathbf{x}_k + \mathbf{v}_k] \tag{10}$$

and by using $\mathbf{v}_{F,k}$ and $H(z) = zH_p(z)$, (10) becomes:

$$\mathbf{w}_k = H_p(z)\big[z[\mathbf{x}_k]\big] + \mathbf{v}_{F,k}. \quad (11)$$

By using Z-transform's time-shift property, i.e., $z[\mathbf{x}_k] = \mathbf{x}_{k+1} + z[\mathbf{x}_0 \cdot \delta(k)]$, where $\delta(k)$ is the discrete delta function, and (3) *under fault-free operation* i.e., $\beta(k - K_0) = 0$, (11) becomes

$$\begin{aligned}\mathbf{w}_k &= H_p(z)\big[\mathbf{x}_{k+1} + z[\mathbf{x}_0 \cdot \delta(k)]\big] + \mathbf{v}_{F,k} \\ &= H_p(z)\big[f(\mathbf{q}_k, \mathbf{x}_k, \mathbf{u}_k) + \eta(\mathbf{q}_k, \mathbf{x}_k, \mathbf{u}_k, k)\big] \\ &\quad + h(k)x_0 + \mathbf{v}_{F,k}. \end{aligned} \quad (12)$$

By also filtering the observer's continuous state estimate $\hat{\mathbf{x}}_k$, given by (6) with initial condition $\hat{\mathbf{x}}_0 = \mathbf{y}_0$, we obtain

$$\hat{\mathbf{w}}_k = H(z)[\hat{\mathbf{x}}_k] \quad (13)$$

By using the filtered output $\mathbf{w}_k$ and the filtered continuous state estimate $\hat{\mathbf{w}}_k$, the residual error to be used for fault detection is given by:

$$\mathbf{r}_k \triangleq \mathbf{w}_k - \hat{\mathbf{w}}_k, \quad (14)$$

and it constitutes the basis of the fault detection scheme. Specifically, a sensor fault is detected by the scheme when $|r_{i,k}| > \bar{R}_{i,k}$, for at least one component i, where $\bar{R}_{i,k}$ is the detection threshold that will be derived in the sequel.

Detection Threshold To derive a suitable nominal detection threshold, we consider the maximum effect of the modeling uncertainty on the residual signal in the case of no sensor faults and also in the absence of any mode mismatches due to autonomous guards events (i.e., $\hat{\mathbf{q}}_k = \mathbf{q}_k$ at all times). By using a similar procedure as in the derivation of (12) and with $\tilde{\mathbf{y}}_k = \mathbf{y}_k$ in (6), $\hat{\mathbf{w}}_k$ from (13) satisfies:

$$\hat{\mathbf{w}}_k = H_p(z)\big[f(\hat{\mathbf{q}}_k, \mathbf{y}_k, \mathbf{u}_k)\big] + h(k)\mathbf{y}_0. \quad (15)$$

Prior to any sensor fault(s) at time step $k < K_0$, the residual error can be written by using equations (12), (15) and (14) as [4]:

$$\mathbf{r}_k = H_p(z)[\Delta f(\mathbf{q}_k, \hat{\mathbf{q}}_k, k) + \eta(\mathbf{q}_k, k)] + \mathbf{v}_{F,k} - h(k)\mathbf{v}_0 \quad (16)$$

where $\Delta f(\mathbf{q}_k, \hat{\mathbf{q}}_k, k)$ is the mismatch function given by:

$$\Delta f(\mathbf{q}_k, \hat{\mathbf{q}}_k, k) \triangleq f(\mathbf{q}_k, \mathbf{x}_k, \mathbf{u}_k) - f(\hat{\mathbf{q}}_k, \mathbf{y}_k, \mathbf{u}_k). \quad (17)$$

By taking the absolute value of (16) component-wise and by using the triangle inequality we obtain for each $i = 1, \ldots, n$:

$$\begin{aligned}|r_{i,k}| \leq |H_p(z)[\Delta f_i(\mathbf{q}_k, \hat{\mathbf{q}}_k, k)]| + |H_p(z)[\eta_i(\mathbf{q}_k, k)]| \\ + |v_{Fi,k}| + |h(k)v_{i,0}|.\end{aligned}$$

To derive a suitable threshold for $|r_{i,k}|$, the following assumption is used:

Assumption 4. The filtered mismatch function in the absence of any mode mismatches is bounded as follows:

$$|H_p(z)[\Delta f_i(\mathbf{q}_k, \hat{\mathbf{q}}_k, k)]| \leq \bar{\Delta} f_i(\hat{\mathbf{q}}_k, k), \ i = 1, \ldots, n \quad (18)$$

where $\bar{\Delta} f_i(\hat{\mathbf{q}}_k, k)$ is a computable bounding function.

Assumption 4 is based on the fact that filtering dampens the measurement noise from the mismatch function $\Delta f_i(\mathbf{q}_k, \hat{\mathbf{q}}_k, k)$. Thus, a suitable selection for $\bar{\Delta} f_i$ can be made through the use of simulations (i.e., Monte Carlo methods) by filtering the mismatch function in all operating modes using the known nominal function dynamics and the available noise characteristics.

Therefore, owing to Assumptions 3 and 4 and also by recalling (9), the following detection threshold can be derived:

$$\bar{r}_{i,k} = \bar{\Delta} f_i(\hat{\mathbf{q}}_k, k) + \bar{H}_p(z)\big[\bar{\eta}_i(\hat{\mathbf{q}}_k)\big] + \bar{v}_{Fi} + |h(k)|\bar{v}_i, \quad (19)$$

where $\bar{H}_p(z)$ is a filter with impulse response $\bar{h}_p(t)$ that satisfies $\bar{h}_p(t) \geq |h_p(t)|$ for all $t \geq 0$ (methods for selecting a suitable filter $\bar{H}_p(z)$ are discussed thoroughly in Keliris et al. (2015)), and $\bar{v}_i$ is a bounding estimate of $v_{i,0}$, i.e., $\bar{v}_i \geq |v_{i,0}|$. Note that the term $|h(k)|\bar{v}_i$ affects the detection threshold only during the initial transient, because the impulse response $h(k)$ of a proper and asymptotically stable transfer function $H(z)$ converges to zero exponentially fast.

The threshold in (19) guarantees no false alarms in the case of no mode mismatches due to autonomous guard event transitions (i.e., $\hat{\mathbf{q}}_k = \mathbf{q}_k$) Therefore, the threshold $\bar{R}_{i,k} = \bar{r}_{i,k}$ is used most of the time in the fault detection scheme. However, to guarantee no false alarms in the case of mode mismatch due to autonomous guard events (i.e., $\hat{\mathbf{q}}_k \neq \mathbf{q}_k$), a new detection threshold $\bar{R}_{i,k} = \bar{r}^*_{i,k}$ is set by the AGEI module when an autonomous guard event is expected to occur. The derivation of the new threshold $\bar{r}^*_{i,k}$ and also the AGEI module are described in the upcoming section 3.3.

3.3 Autonomous Guard Events Identification (AGEI)

Because of the presence of autonomous guard events triggered by the continuous state values $\mathbf{x}$, and the availability in the observer of only the output values $\mathbf{y}$ that include measurement noise, the observer can trigger these autonomous guard events at a different time step than the system, causing mode mismatch (i.e., $\hat{\mathbf{q}}_k \neq \mathbf{q}_k$) and subsequently false alarms. To exclude the possibility of such false alarms and also to trigger these events effectively in the observer, the AGEI module is used. Specifically, the AGEI module monitors for autonomous guard events in the system. If it determines that an autonomous guard event is expected to occur, it calculates and sets a new detection threshold in the fault detection scheme to avoid any potential false alarms. Moreover, the AGEI module can identify if the expected autonomous guard event has indeed occurred in the system and subsequently trigger it in the observer allowing effective mode estimation.

For performing the above operations, the AGEI module uses the AGEI Matrix, which keeps in each row all the necessary details for every autonomous guard event g_{aj}, $j = 1, \ldots, n_{g_a}$ in the system. Specifically, for each g_{aj} it keeps: (a) the enabling mode q_{Ij} which is the mode of subsystem I from which g_{aj} can be triggered, (b) the enabling condition $x_i \triangle_j \xi_{aj}$ that triggers g_{aj}, (c) the transition mode q^*_{Ij} which is the mode that that subsystem I transitions after g_{aj} is triggered, and finally (d) the residual(s) $r_i \ \forall i$ affected by g_{aj}.

Moreover, we consider that there is a *dwell-time* between consecutive autonomous guard events, as in Hespanha and Morse (1999). Thus, only one autonomous guard event

[4] In the rest of the paper, when there is no risk of ambiguity, and for the sake of simplicity, a compact notation like $\eta(\mathbf{q}_k, k) \equiv \eta(\mathbf{q}_k, \mathbf{x}_k, \mathbf{u}_k, k)$ and $\Delta f(\mathbf{q}_k, \hat{\mathbf{q}}_k, k) \equiv \Delta f(\mathbf{q}_k, \hat{\mathbf{q}}_k, \mathbf{x}_k, \mathbf{y}_k, \mathbf{u}_k)$ will be used.

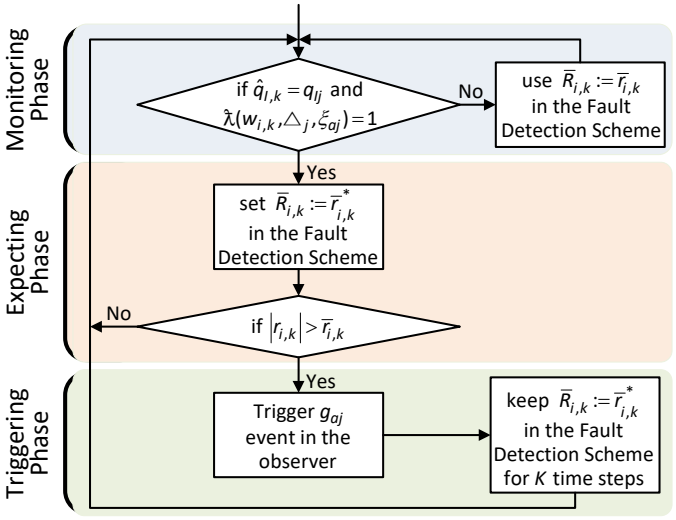

Fig. 3. AGEI algorithm diagram.

occurs at each time. Finally, to guarantee correct mode estimation by the AGEI in case of a sensor fault, we consider that the necessary time for learning the sensor fault magnitude is always less than the dwell-time of consecutive autonomous guard events. A diagram for AGEI algorithm is shown in Fig. 3 and consists of three main sequential phases, namely Monitoring, Expecting, and Triggering, that we describe in the following paragraphs.

Monitoring Phase Based on the estimated mode $\hat{\mathbf{q}}_k$ and the filtered measurements $\mathbf{w}_k$, the AGEI monitors if any autonomous guard event g_{aj} is possible to occur. Specifically, to accomplish this, the algorithm makes the following checks (see Fig. 3): (a) if the current mode estimate $\hat{q}_{I,k}$ matches the enabling mode q_{Ij} for the g_{aj}, and (b) if the function $\lambda(\cdot)$ returns 1. The first check determines if g_{aj} is possible to occur based on the current mode estimate. The second check determines if g_{aj} is possible to occur based on its enabling condition $x_i \triangle_j \xi_{aj}$. In more detail, $\lambda(w_{i,k}, \triangle_j, \xi_{aj})$ uses the decision rule:

$$\lambda(\cdot) = \begin{cases} & \text{if } \Xi^-_{aj} \leq |w_{i,k}| \leq \Xi^+_{aj} \text{ and } \triangle_j \in \{=\} \\ 1 & \text{if } |w_{i,k}| \geq \Xi^-_{aj} \text{ and } \triangle_j \in \{>, \geq\} \\ & \text{if } |w_{i,k}| \leq \Xi^+_{aj} \text{ and } \triangle_j \in \{<, \leq\} \\ 0 & \text{otherwise} \end{cases} \quad (20)$$

where Ξ^+_{aj} and Ξ^-_{aj} bounds are calculated by:

$$\Xi^{\pm}_{aj} \triangleq (1 \pm \delta) \left| H(z)[\xi_{aj}] \right|. \quad (21)$$

The decision rule in (20) relies on the filtered measurement $w_{i,k}$ and the filtered value of ξ_{aj} from the enabling condition. Also, the filtered noise and the delay that the filtering imposes, are taken into consideration by incorporating the design parameter constant $\delta \in (0, 1]$ that determines the percentage to set Ξ^+_{aj} up and Ξ^-_{aj} down from $H(z)[\xi_{aj}]$, as indicated by (21). In this way, the AGEI module can anticipate the guard event g_{aj} before it occurs, so that it can set the new detection threshold accordingly. The value of δ can be initially set around 5% and can be further fine-tuned by observing when the new detection threshold is applied in the Fault Detection scheme. If any or both the above checks are false, then the algorithm determines that the autonomous guard event g_{aj} will not occur in the system; thus, the nominal detection threshold that is given in (19), i.e., $\bar{R}_{i,k} = \bar{r}^*_{i,k}$, is used in the Fault Detection scheme. However, if both checks are true, then the algorithm determines that the autonomous guard event g_{aj} is possible to occur and it continues to the Expecting phase.

Expecting Phase As can be seen in the expecting phase in Fig. 3, the AGEI first set in the Fault Detection scheme a new detection threshold $\bar{R}_{i,k} = \bar{r}^*_{i,k}$ for any residual(s) affected by g_{aj}, according to the AGEI Matrix. The new detection threshold considers the mode mismatch error between system and observer, due to the expected g_{aj}, as well as the maximum bound on the modeling uncertainty between either the current mode or the transitioning mode. Thus, by following a similar procedure as in the derivation of (19), the new detection threshold is given by:

$$\bar{r}^*_{i,k} = \bar{\Delta} f_i(\mathbf{q}^*_k, \hat{\mathbf{q}}_k, k) + \bar{H}_p(z)\left[\bar{\eta}^*_i\right] + \bar{v}_{Fi,k} + |h(k)|\bar{v}_i, \quad (22)$$

where $\mathbf{q}^*$ is the new mode that the system transitions if g_{aj} occurs (according to AGEI Matrix), $\bar{\Delta} f_i(\mathbf{q}^*_k, \hat{\mathbf{q}}_k, k)$ is the *mode* mismatch bounding function that can be obtained similar to Assumption 4, and finally, the uncertainty bound $\bar{\eta}^*_i$ is calculated using $\bar{\eta}^*_i \triangleq \max\left(\bar{\eta}_i(\hat{\mathbf{q}}_k, k), \bar{\eta}_i(\hat{\mathbf{q}}^*_k, k)\right)$. The new detection threshold given in (22) is larger or equal than the nominal threshold, i.e., $\bar{r}^*_{i,k} \geq \bar{r}_{i,k}$, and it guarantees no false alarms due to possible mode mismatches because of expected autonomous guard events g_{aj}.

With the new detection threshold set, the algorithm works on identifying if g_{aj} has occurred in the system. This is done by checking if the residual signal that is affected by g_{aj} has crossed its corresponding nominal threshold, i.e., $|r_{i,k}| > \bar{r}_{i,k}$. This is based on the fact that after a mode change in the system due to g_{aj}, there will be an increase in the residual signal because of the occurred mode mismatch, and it will be detected once it crosses its corresponding threshold.

Triggering Phase Once it is determined that g_{aj} has occurred in the system, the AGEI algorithm moves to the triggering phase, shown in Fig. 3. The AGEI first triggers the anticipated autonomous guard event g_{aj} in the hybrid automaton observer. Next, the AGEI algorithm keeps the new threshold given by (22) in the Fault Detection scheme for the next K time steps. This is necessary for avoiding any false alarms due to transients in the residual signal because of mode change in the observer, which are picked up by the filters. The number of the necessary time steps K is equal to the number of time steps that the impulse response of $h(k)$ takes to converge to zero (or sufficiently close to zero in the case of IIR filter). After the K time steps are passed, the AGEI algorithm returns to the monitoring phase and monitors again for autonomous guard events.

3.4 Adaptive Sensor Bias Fault Estimation

When a fault is detected at time step $k = K_d$, the following estimation model is activated to estimate the magnitude of the sensor bias fault(s)

$$\hat{\mathbf{x}}^s_{k+1} = f(\hat{\mathbf{q}}_k, \hat{\mathbf{x}}^s_k, \mathbf{u}_k) + \Lambda \epsilon^s_k, \quad \hat{\mathbf{x}}^s_{K_d} = \mathbf{y}_{K_d} \quad (23)$$

$$\hat{\mathbf{y}}^s_k = \hat{\mathbf{x}}^s_k + \hat{\boldsymbol{\sigma}}_k \quad (24)$$

$$\hat{\boldsymbol{\sigma}}_{k+1} = \hat{\boldsymbol{\sigma}}_k + \mathcal{P}_{\boldsymbol{\sigma}}[\Gamma \epsilon^s_k], \quad \hat{\boldsymbol{\sigma}}_{K_d} = 0 \quad (25)$$

where $\boldsymbol{\epsilon}_k^s \triangleq \mathbf{y}_k - \hat{\mathbf{y}}_k^s$ denotes the output estimation error, Λ is a design matrix that is selected so that is Schur stable, and $\hat{\boldsymbol{\sigma}} \in \mathbb{R}^n$ denotes the sensor fault estimation vector. Finally, $\mathcal{P}_\sigma[\cdot]$ is a projection operator that restrains the estimation vector $\hat{\boldsymbol{\sigma}}$ in a predefined and convex region $\Theta_\sigma \in \mathbb{R}^n$ to guarantee the stability of the learning algorithm in the presence of noise and modeling uncertainty. In this paper, Θ_σ is considered to be a zero-origin hypersphere of radius M_σ, with the projection operator in (25) to be given by Keliris et al. (2017)

$$\mathcal{P}_\sigma[\Gamma\epsilon_k^s] = \begin{cases} \Gamma\boldsymbol{\epsilon}_k^s - \Gamma\frac{\hat{\boldsymbol{\sigma}}_k\hat{\boldsymbol{\sigma}}_k^T}{\hat{\boldsymbol{\sigma}}_k^T\Gamma\hat{\boldsymbol{\sigma}}_k}\Gamma\boldsymbol{\epsilon}_k^s & \text{if } |\hat{\boldsymbol{\sigma}_k}| \geq M_\sigma \text{ and} \\ & \hat{\boldsymbol{\sigma}_k}^T\Gamma\boldsymbol{\epsilon}_k^s > 0. \\ \Gamma\boldsymbol{\epsilon}_k^s, & \text{otherwise} \end{cases} \tag{26}$$

where $\Gamma \in \mathbb{R}^{n\times n}$ is a symmetric and positive definite learning rate matrix. Note that the adaptive estimation model above estimates the sensor fault magnitudes for all the sensors in the system. Thus, the sensor fault estimates $\hat{\boldsymbol{\sigma}}$ can be used to recognize which sensors are healthy and which are faulty. In the case of healthy sensors, their sensor bias fault estimates values will eventually converge close to zero, while for faulty sensors, this will not be the case. Also, as explained earlier in Section 3.1, the sensor fault estimates are used for canceling the actual sensor faults, which allows both the hybrid observer and AGEI module to continue their correct function even in the presence of sensor faults.

4. CONCLUSION

In this paper, a sensor bias fault diagnosis approach for a class of nonlinear uncertain hybrid systems is proposed. An observer based on a modified hybrid automaton framework is used to estimate the hybrid state while a filtering approach is employed in the fault detection scheme that allows tighter mode-dependent thresholds while guaranteeing no false alarms. An autonomous guard events identification (AGEI) module is developed to eliminate any false alarms due to autonomous guard event and also enable effective mode estimation in the observer. Lastly, an adaptive sensor fault estimation scheme is activated once a fault is detected to estimate the sensor bias fault(s) magnitudes that are then used to compensate the measurements so that both the observer and AGEI module can continue their operation. Future research efforts will be devoted to the designing of a modeling uncertainty learning approach along with a comprehensive fault diagnosis architecture for uncertain nonlinear systems that will handle discrete and parametric faults along with sensor faults.

ACKNOWLEDGEMENTS

This work has been supported by the European Union's Horizon 2020 research and innovation programme under grant agreement No 739551 (KIOS CoE).

REFERENCES

Bayoudh, M., Travé-Massuyès, L., and Olive, X. (2008). Hybrid Systems Diagnosis by coupling Continuous and Discrete event Techniques. *Proc. IFAC World Congress*, 7265–7270.

Cocquempot, V., Mezyani, T.E., and Staroswiecki, M. (2004). Fault detection and isolation for hybrid systems using structured parity residuals. In *2004 5th Asian Control Conference*, volume 2, 1204–1212.

Daigle, M., Bregon, A., and Roychoudhury, I. (2016). A Qualitative Fault Isolation Approach for Parametric and Discrete Faults Using Structural Model Decomposition. In *Annual Conference of the PHME16*.

Heracleous, C., Keliris, C., Panayiotou, C.G., and Polycarpou, M.M. (2018a). Centralized Fault Detection of Complex Uncertain Hybrid Systems. *IFAC-PapersOnLine*, 51(7), 76–81. WODES 2018.

Heracleous, C., Kolios, P., Panayiotou, C.G., Ellinas, G., and Polycarpou, M.M. (2017). Hybrid systems modeling for critical infrastructures interdependency analysis. *Reliability Engineering & System Safety*, 165, 89 – 101.

Heracleous, C., Panayiotou, C.G., and Polycarpou, M.M. (2018b). Fault Diagnosis of Uncertain Hybrid Systems. *IFAC-PapersOnLine*, 51(24), 123–130. SAFEPROCESS 2018.

Hespanha, J.P. and Morse, A.S. (1999). Stability of switched systems with average dwell-time. In *Proc. of the 38th IEEE CDC*, 2655–2660 vol.3.

Hofbaur, M.W. and Williams, B.C. (2004). Hybrid estimation of complex systems. *IEEE Trans. on Systems, Man, and Cybernetics, Part B*, 34(5), 2178–2191.

Keliris, C., Polycarpou, M.M., and Parisini, T. (2017). An Integrated Learning and Filtering Approach for Fault Diagnosis of a Class of Nonlinear Dynamical Systems. *IEEE Trans. on Neural Networks and Learning Systems*, 28(4), 988–1004.

Keliris, C., Polycarpou, M.M., and Parisini, T. (2018). An Adaptive Approach to Sensor Bias Fault Diagnosis and Accommodation for a Class of Input-Output Nonlinear Systems. In *2018 IEEE CDC*, 6334–6339.

Keliris, C., Polycarpou, M.M., and Parisini, T. (2015). Distributed fault diagnosis for process and sensor faults in a class of interconnected input-output nonlinear discrete-time systems. *Int. Journal of Control*, 88(8), 1472–1489.

Narasimhan, S. and Biswas, G. (2007). Model-Based Diagnosis of Hybrid Systems. *IEEE Trans. on Systems, Man, and Cybernetics - Part A: Systems and Humans*, 37(3), 348–361.

Reppa, V., Polycarpou, M.M., and Panayiotou, C.G. (2014). Adaptive Approximation for Multiple Sensor Fault Detection and Isolation of Nonlinear Uncertain Systems. *IEEE Transactions on Neural Networks and Learning Systems*, 25(1), 137–153.

Vemuri, A.T. (2001). Sensor bias fault diagnosis in a class of nonlinear systems. *IEEE Transactions on Automatic Control*, 46(6), 949–954.

Wang, W., Li, L., Zhou, D., and Liu, K. (2007). Robust state estimation and fault diagnosis for uncertain hybrid nonlinear systems. *Nonlinear Analysis: Hybrid Systems*, 1(1), 2–15.

Zhang, X., Parisini, T., and Polycarpou, M.M. (2005). Sensor bias fault isolation in a class of nonlinear systems. *IEEE Trans. on Automatic Control*, 50(3), 370–376.

Zhao, F., Koutsoukos, X., Haussecker, H., Reich, J., and Cheung, P. (2005). Monitoring and fault diagnosis of hybrid systems. *IEEE Trans. on Systems, Man, and Cybernetics, Part B (Cybernetics)*, 35(6), 1225–1240.